Ray-optics study of gentle non-conformal texture morphologies for perovskite/silicon tandems

Santbergen, Rudi; Vogt, Malte R.; Mishima, Ryota; Hino, Masashi; Uzu, Hisashi; Adachi, Daisuke; Yamamoto, Kenji; Zeman, Miro; Isabella, Olindo

DOI
10.1364/OE.448545

Publication date
2022

Document Version
Final published version

Published in
Optics Express

Citation (APA)
Santbergen, R., Vogt, M. R., Mishima, R., Hino, M., Uzu, H., Adachi, D., Yamamoto, K., Zeman, M., & Isabella, O. (2022). Ray-optics study of gentle non-conformal texture morphologies for perovskite/silicon tandems. *Optics Express*, *30*(4), 5608-5617. https://doi.org/10.1364/OE.448545

Research Article Vol. 30, No. 4 / 14 Feb 2022 / Optics Express 5608
Optics EXPRESS

Ray-optics study of gentle non-conformal texture morphologies for perovskite/silicon tandems

RUDI SANTBERGEN,[1,*] MALTE R. VOGT,[1] RYOTA MISHIMA,[2,3] MASASHI HINO,[3] HISASHI UZU,[3] DAISUKE ADACHI,[3] KENJI YAMAMOTO,[3] MIRO ZEMAN,[1] AND OLINDO ISABELLA[1]

[1]*Photovoltaic Materials and Devices, TU Delft, 2628 CD, Delft, Netherlands*
[2]*KANEKA Belgium N.V., 2260 Westerlo-Oevel, Belgium*
[3]*KANEKA Corporation, Settsu, Osaka 566-0072, Japan*
[*]*r.santbergen@tudelft.nl*

Abstract: We investigate gentle front side textures for perovskite/silicon tandem solar cells. These textures enhance the absorption of sunlight, yet are sufficiently gentle to allow deposition of an efficient perovskite top cell. We present a tandem solar cell with such gentle texture, fabricated by Kaneka corporation, with an efficiency as high as 28.6%. We perform an extensive ray-optics study, exploring non-conformal textures at the front and rear side of the perovskite layer. Our results reveal that a gentle texture with steepness of only 23° can be more optically efficient than conventional textures with more than double that steepness. We also show that the observed anti-reflective effect of such gentle textures is not based a double bounce, but on light trapping by total internal reflection. As a result, the optical effects of the encapsulation layers play an important role, and have to be accounted for when evaluating the texture design for perovskite/silicon tandems.

1. Introduction

Surface textures are indispensable for enhancing the absorption of sunlight in solar cells [1]. For conventional monocrystalline silicon wafer based solar cells, the pyramid texture is the industry standard, as it combines optical effectiveness with ease of fabrication. This texture is fabricated by a wet-etching process that preferentially etches specific crystal planes, resulting in pyramids that have a steepness of about 51° [2]. This steepness, being larger than 45°, guarantees that an incoming light ray undergoes at least two bounces, which reduces the reflectance loss significantly. Note that for a solar cell encapsulated behind glass, a second bounce is already guaranteed for a pyramid steepness of only 21°, as reflected light falls outside the critical angle at glass/air interface and is guaranteed to return to the silicon surface after total internal reflection [3]. More details are given in supplement S1.

Two-terminal perovskite / silicon tandem solar cells [4] have recently demonstrated power conversion efficiencies close to 30% [5–6], exceeding the efficiency limit of conventional silicon solar cells [7–8]. These tandems, currently being developed in the lab, are expected to enter the market within a few years and then steadily increase their market share [9]. Fabrication of these two-terminal perovskite / silicon tandem cells is done by depositing a thin-film perovskite top cell, directly on top of a wafer based silicon bottom cell. It is challenging to fabricate the perovskite cell on top of the conventional pyramid texture. Therefore most tandem devices fabricated today are based on front-side polished silicon wafers, providing a flat, albeit more reflective, substrate for perovskite top cell deposition. Optical simulation studies have shown that tandems that do have front side pyramid texture would suffer significantly less reflection losses [10–12]. Therefore efforts are ongoing to develop robust perovskite deposition methods

#448545 https://doi.org/10.1364/OE.448545
Journal © 2022 Received 18 Nov 2021; revised 12 Jan 2022; accepted 17 Jan 2022; published 7 Feb 2022

Optics EXPRESS

for textured surfaces [13], as well as efforts to explore more gentle, smaller and less steep surface textures [14], suitable for conventional perovskite deposition methods, yet optically efficient. Good layer growth and tandem efficiency have already been demonstrated with blade-coating [15] or solution processing [16] of perovskite on relatively small pyramid texture, which typical feature size in the range of 1 to 2 µm.

Optimization of textured perovskite / silicon tandems requires optical models that can treat both coherent and incoherent layers, as well as light scattering and trapping effects due to texture. Simulation studies frequently use hybrid models [17–19] and often assume that silicon front surface is either flat or has the conventional pyramid texture. Usually also the perovskite top cell is assumed to be conformal, i.e. all interfaces follow exactly the underlying texture morphology, and the effects of encapsulation are usually not considered. Gentle texture morphologies for tandems have been studied using Maxwell solvers [14]. However, due to the high computational cost, simplifying assumptions have to be made regarding the back reflector at the rear side of the silicon wafer, and only a limited number of cases can be considered. Thus far, there has not been an extensive study on the optical effects of gentle textures of reduced steepness in combination with non-conformal perovskite top cells and encapsulation.

In this work, we present an extensive study on the effect of texture steepness on reflection losses in the two-terminal perovskite / silicon tandem. We limit ourselves to sufficiently large ($>$ 1 µm) textures for which ray optics is applicable. To analyze the effects of non-conformal perovskite top cells, we simulate all combinations of texture steepness at the front and rear side of the perovskite layer. The goal of this analysis is to explore how these gentle, non-conformal textures enhance the implied photocurrent of the perovskite and silicon absorber layers, both without and with encapsulation layers present.

2. Method

In this section we discuss the optical model and the input parameters used for simulation of perovskite / silicon tandems with gentle textures. We also validate the model by comparing simulation results to measurements.

2.1. GenPro4 optical model

For this study we use the GenPro4 optical model, developed in-house [17]. The GenPro4 optical model represents a solar cell as a stack of *thick* layers, where each interface can contain a stack of *thin* coatings, giving rise to interference, and a surface texture that can reduce reflection and scatter light. Each interface is optically characterized by a so-called scatter matrix and all scatter matrices are combined into a set of equations that is solved to obtain the overall reflectance R, absorptance A and transmittance T of the device [17]. An advantage of this algorithm, as opposed to ray tracing the entire device at once, is that scatter matrices of individual interfaces can be saved, reused and combined. For this specific study, where many combinations of perovskite front and rear side textures are simulated, this algorithm reduces computation time by orders of magnitude [17,20].

2.2. Input parameters

Input for the simulations are the thickness of each layer, the corresponding optical constants (n and k) and the texture morphologies of the interfaces. The incoming light is normally incident. We perform the optical simulations for a two-terminal perovskite / silicon tandem device structure similar to the 29.15% efficient tandem by Al-Ashouri et al. [6]. Further details about the device structure and fabrication process can be found in the supplementary material of Ref. 6. The layers and their thicknesses used for our simulations are indicated in Fig. 1(a). The optical constants n and k were either measured in house or taken from literature. In our simulations we consider three interfaces labelled 1, 2 and 3 (see Fig. 1(a)) with distinct texture morphologies. The perovskite top

Optics EXPRESS

cell is conformal when the morphologies of interfaces 1 and 2 are identical, and non-conformal when they differ. The thickness of a non-conformal layer varies from point to point, and in our simulations the specified thickness is the average thickness or volume thickness, i.e. the thickness that a flat layer with the same volume of material would have. For interfaces 1 and 2 we will consider gentle textures, while for interface 3 we always use the conventional pyramid texture with a steepness $\chi_3 = 51°$. In the simulations, the texture morphologies are discretized into tiny triangular mesh elements and we define texture steepness χ, as these elements' average slope. The anti-reflective and light scattering effects of textures are then modelled using the built-in ray-tracing model of GenPro4, which takes as input the height map of the texture morphology, for example obtained from atomic force microscopy. For interfaces 1 and 2 we will vary steepnesses χ_1 and χ_2 numerically, by multiplying the height data with a constant factor. As output, the simulation gives the absorptance in each layer as a function of wavelength. To analyze reflection losses, we decompose the total reflectance R_{tot} into reflection components R_1, R_2 and R_3 by first simulating just interface 1 (which gives R_1), then interfaces 1 till 2 (which gives $R_1 + R_2$) and finally interfaces 1 till 3 (which gives $R_{tot} = R_1 + R_2 + R_3$).

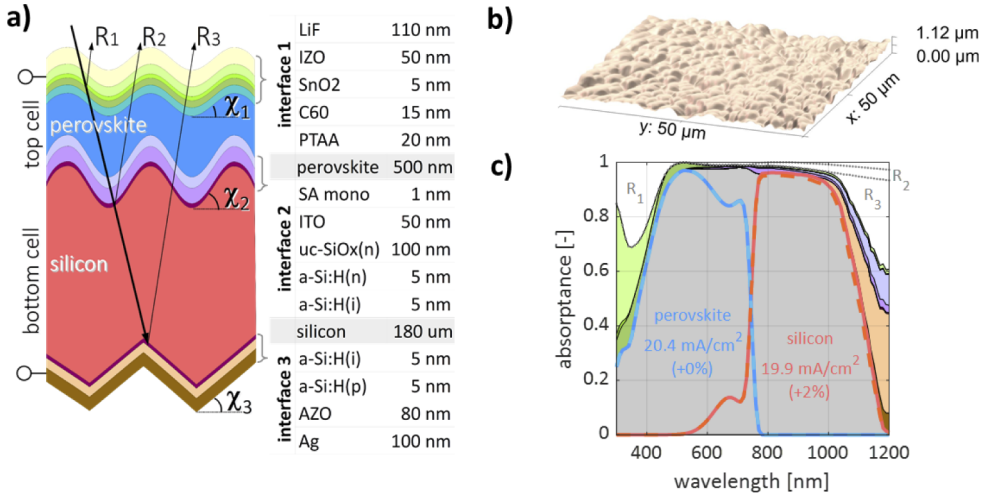

Fig. 1. a) Cross-section of the simulated tandem, with interfaces 1, 2 and 3, the corresponding texture steepness values (χ_1, χ_2 and χ_3) and reflection components (R_1, R_2 and R_3) indicated. b) Gentle texture height map, measured by AFM, used as input for the simulation. c) Simulated reflectance (white) and absorptance in each layer (colors match Fig. 1(a)) as a function of wavelength for tandem with above mentioned gentle texture ($\chi_1 = \chi_2 = 10°$). Blue and red lines represent useful absorptance in perovskite and silicon, with dashed lines for the front flat ($\chi_1 = \chi_2 = 0°$) reference case.

2.3. *Experimental validation*

Next we optically simulate the gently textured tandem shown in Fig. 1(a). The gentle texture morphology shown in Fig. 1(b) was fabricated by wet chemical etching of the silicon wafer. An etching method similar to the one described by ref. 21 was used. The resulting texture was measured by atomic force microscopy (AFM). From the obtained slope distribution, given in supplement S2, it is clear that with an average slope of 10° this texture is indeed very gentle. The measured AFM data was used as input in the simulations and applied to interface 2, so $\chi_2 = 10°$. We assume the 500 nm perovskite layer is conformal so that interface 1 has the same texture ($\chi_1 = 10°$). The simulation result is shown in Fig. 1(c). The reflection losses R_1, R_2 and R_3 are indicated in white. The parasitic absorption losses at the shorter wavelengths are dominated by

Optics EXPRESS

IZO (light green) and C60 (dark green) and at the longer wavelengths by ITO (purple) and AZO (orange). The useful absorptance (gray) consists of contributions from perovskite (blue line) and silicon (red line). By integrating these absorptances over the AM1.5 solar spectrum, a J_{ph} of 20.4 and 19.9 mA/cm^2 are obtained for perovskite and silicon, respectively. For reference, this tandem was also simulated with a flat top cell ($\chi_1 = 0°$, $\chi_2 = 0°$) while keeping the rear texture fixed ($\chi_3 = 51°$). The reference absorptance in perovskite and silicon are shown in Fig. 1(c) as dashed lines. The comparison reveals that going from flat to gently textured top cell hardly affects the J_{ph} of perovskite (+0%), but does slightly increase in the J_{ph} of silicon (+2%). In section 3 we will show that further enhancements are possible by optimizing the gentle texture.

Tandem devices were also fabricated. This was done once with flat top cell and once with a gently textured top cell, based on the texture shown in Fig. 1(b). Figure 2(a) shows one minus measured reflectance 1-*R* (black) and the external quantum efficiency EQE measured for top cell (blue) and bottom cell (red). The dashed lines are used for the tandem with flat top cell and solid lines for the tandem with gently textured top cell. This shows that the gentle texture reduces reflection and correspondingly enhances top and bottom cell EQE. As a result, the top cell current has increased by +1.1% (from 19.57 to 19.78 mA/cm^2) and the bottom cell current has increased by +1.4% (from 19.19 to 19.46 mA/cm^2). To demonstrate the potential of the gentle surface texture, the JV-curves of the gently textured tandem are shown in Fig. 2(b), once measured in forward (fwd) and once in reverse (rev) direction. The measured efficiency (average of forward and reverse scan) is as high as 28.6%.

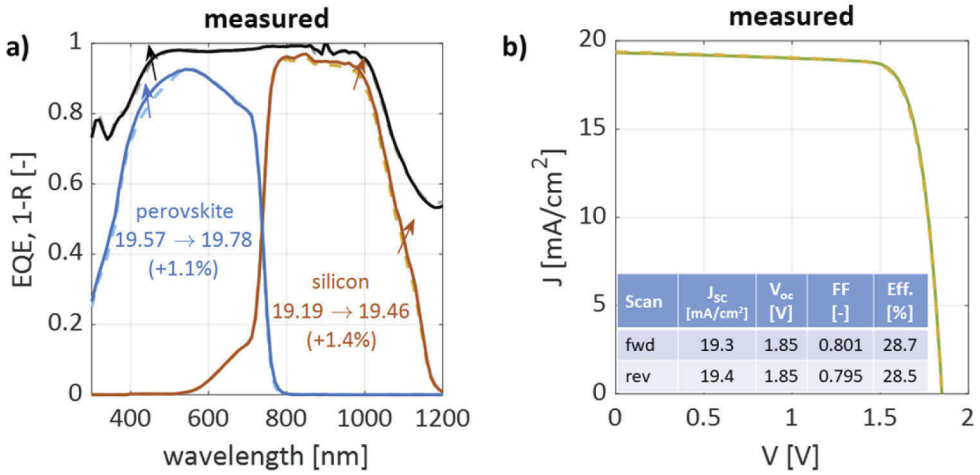

Fig. 2. a) Measured EQE of top and bottom cell (blue and red lines) and 1-*R* (black line) for tandem with gentle texture (solid lines) and flat reference (dashed lined). b) Measured JV-curve in forward (green) and reverse (orange) scan direction of tandem with gentle texture. The inset shows the measured external parameters.

Comparing the measurements of Fig. 2(a) to the simulations of Fig. 1(c), we see there is a good agreement. On average there is less than 3% deviation between on the one hand measured reflectance and top/bottom cell EQE and on the other hand simulated reflectance and perovskite/silicon absorptance. The slight reflection reduction and corresponding EQE enhancement due to texture, observed experimentally at the shorter wavelengths (400 to 600 nm), is not observed in the simulation, but could be explained if for the gently textured case the front window layers would be slightly thinner compared to the flat case. The slight enhancement in silicon bottom cell EQE is observed in both experiment and simulation. Here we point out that a part of the experimentally observed enhancement is due to the c-Si bottom cell being slightly thicker for the gently textured case (190 versus 176 μm). Because enhancement effects are subtle

Optics EXPRESS

and experimentally layer thickness are hard to reproduce within a few percent accuracy, in section 3 we continue the optical study of gentle texture morphologies using simulations only.

3. Simulation results

In this section we use the GenPro4 model to study the effect of gentle textures at interfaces 1 and 2 on the optical losses. We keep all layer thickness fixed at the values indicated in Fig. 1(a). In addition we also consider encapsulated devices that have additional 450 µm of polyolefin and 3.2 mm of glass at their front side, which is more representative for real-world outdoor applications. Note that for the encapsulated tandems the LiF anti-reflective coating was moved from the IZO layer to the front side of the encapsulation glass. The gentle textures are represented by pyramids of variable steepness. Pyramid texture was used because all elements of a pyramid have the same steepness, which makes the analysis of the simulation results more straightforward. A more rounded texture, like the one shown in Fig. 1(b), exhibits some spread in the elements' slope (see supplement S2). We fix the width of the pyramid base to 2 µm and vary the pyramid height to attain the desired steepness. Note that the ray-optics based simulation results presented here do not depend on the absolute size of the pyramids, merely on their steepness, and are therefore rather general. However, ray-optics is not accurate for small sub-wavelength pyramids, for which wave effects like diffraction are dominant. First we consider the special case that the perovskite top cell is conformal, i.e. interfaces 1 and 2 have identical textures ($\chi_1 = \chi_2$). Then in section 3.2, we consider the non-conformal case and vary χ_1 and χ_2 independently. Note that in all cases the rear pyramid texture remains fixed at $\chi_3 = 51°$.

3.1. Conformal top cell

The tandem shown in Fig. 1(a) is simulated while texture steepnesses χ_1 and χ_2 are varied simultaneously between 0° and 60°, in steps of 1°. Figure 3(a) shows, as a function of $\chi_1 = \chi_2$, the reflection losses (white) and parasitic absorption loss in each layer (colors, corresponding to Fig. 1). The gray area indicates the remaining useful implied photocurrent density, i.e. the sum of perovskite and silicon currents. For the front-side flat reference device ($\chi_1 = \chi_2 = 0°$), the useful photocurrent is 39.9 mA/cm^2, in agreement with the results already presented in Fig. 1(c) (dashed lines). The main optical losses are reflectance losses R_1, R_2, R_3 and parasitic absorption loss in IZO, C60, ITO, uc-Si and AZO layers. By increasing texture steepness to a moderate 15°, the useful photocurrent is increased by about 1.3% (to 40.5 mA/cm^2). Figure 3(a) shows that this is largely due to a reduction of reflection loss R_2, i.e. improved incoupling of light transmitted by perovskite into silicon (see Fig. 1(a)). Further increasing texture amplitude has no benefit, until at a steepness of about 40°, reflection loss R_1 is being reduced as well. We attribute this to improved incoupling of light from air into perovskite due to double bounces. This ultimately increases useful photocurrent, relative to the front side flat device, by 2.5% (to 41.0 mA/cm^2). Interestingly, the other optical losses are hardly affected by texture steepness.

The simulation results for the same tandem, but with additional glass/polyolefin encapsulation layers, is shown in Fig. 3(b). Compared to the unencapsulated case, there are additional reflection losses at the air/glass interface (R_0) and parasitic absorption losses in both glass and polyolefin (indicated in light gray). As a result, the useful photocurrent density is now 'only' 38.3 mA/cm^2 for the front-flat reference case. As before, increasing the texture steepness reduces both R_2 and R_1, thereby increasing the useful photocurrent, without much affecting the other losses. Interestingly, for a moderate texture steepness of only 23°, both R_1 and R_2 are already reduced from more than 1 mA/cm^2 to nearly zero, increasing the useful photocurrent by as much as 3.3% (to 39.6 mA/cm^2). Note that 23° steepness is sufficient for reducing R_1, because all light reflected by this moderate texture will undergo total internal reflection at the glass/air interface and is guaranteed to return for a second bounce. Further increasing the texture steepness only increases the optical losses and reduces the useful photocurrent. This shows firstly that when designing

Optics EXPRESS

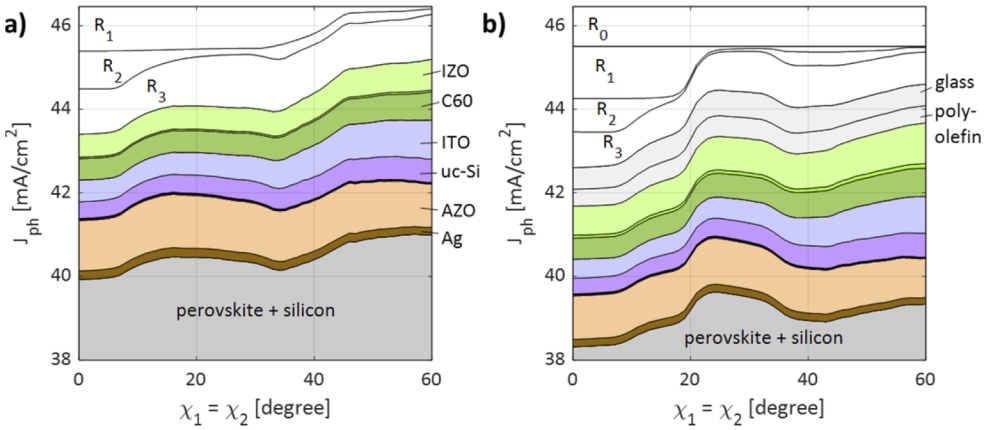

Fig. 3. Simulated reflectance loss (white), parasitic absorptance loss (colors) and remaining useful photocurrent in perovskite plus silicon (gray), all expressed in mA/cm^2, as a function of texture steepness $\chi_1 = \chi_2$. a) for the unencapsulated tandem. b) for the encapsulated tandem.

tandem texture, the effect of encapsulation has to be accounted for, and secondly that a relatively gentle texture steepness of only 23° maximizes the useful photocurrent by means of total internal reflection.

3.2. *Non-conformal top cell*

Next, we simulate again the tandem shown in Fig. 1(a), but now with texture steepness χ_1 different from χ_2. In practice, such unequal steepnesses will occur when perovskite top cell deposition is non-conformal. The simulations are performed for every combination of χ_1 and χ_2, ranging from 0° to 60° in steps of 1°, so for $61 \times 61 = 3721$ simulations in total. Note that because the scatter matrices calculated for the results presented in section 3.1 could be reused (as explained in section 2.1), each simulation spanning the wavelength range 300 to 1200 nm, is performed within only a few seconds on a typical CPU.

The simulated implied photocurrents of the perovskite and silicon absorber layers are shown as a contour plot in Fig. 4, where the percentages represent the current gain relative to the front side flat device ($\chi_1 = \chi_2 = 0°$). We first discuss the results for the unencapsulated tandem, shown on the left. Figure 4(a) shows that the implied photocurrent of the *perovskite* increases steadily when increasing χ_1. This corresponds to a steady decrease in reflection loss R_1 (see supplement S3), as well as light traveling a more oblique path through the perovskite, increasing the optical thickness of this layer. However, it does not depend strongly on χ_2. A texture steepness of more than 30° is required to achieve a perovskite current gain of over 2%. On the other hand, the implied photocurrent of the *silicon* shows a distinct maximum, with a gain of over 3% around $\chi_1 = 0°$, $\chi_2 = 20°$ (see Fig. 4(b)). This is caused by reduction of reflection loss R_2 (see supplement S3). This particular steepness combination maximizes the probability of any light reflected at the perovskite / silicon interface to return to the silicon after undergoing total internal reflection (TIR) at the perovskite / air interface, as schematically illustrated in Fig. 4(c).

The simulation results for the encapsulated tandem are shown in the right column of Fig. 4. Although the trends are the same, important shifts can be observed. As shown in Fig. 4(d), enhancing perovskite photocurrent by more than 2% now requires a texture steepness χ_1 of only 22°. This is because total internal reflection at the glass/air interface guarantees a second bounce that reduces R_1 even for moderately steep textures. Figure 4(e) shows that the implied photocurrent in silicon still has the original maximum around $\chi_1 = 0°$, $\chi_2 = 20°$. However, this

Optics EXPRESS

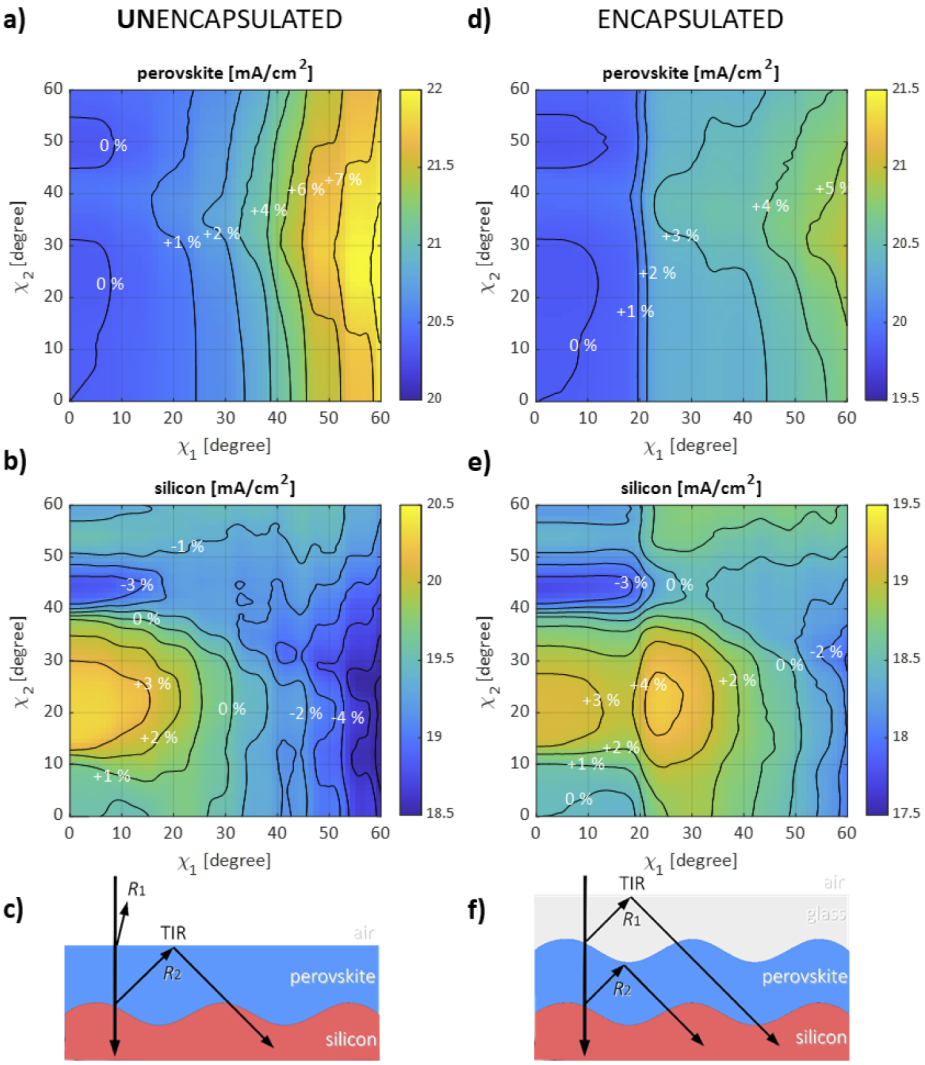

Fig. 4. Implied photocurrent in perovskite and silicon for every combination of texture steepness χ_1 and χ_2 for the unencapsulated (left) and encapsulated tandem (right). a) perovskite in unencapsulated tandem, b) silicon in unencapsulated tandem, c) mechanism for enhancing silicon photocurrent in unencapsulated tandem. d) perovskite in encapsulated tandem, e) silicon in encapsulated tandem, f) mechanism for enhancing silicon photocurrent in encapsulated tandem.

now is only a local maximum as an even larger gain of over 4% can be obtained for $\chi_1 = 23°$, $\chi_2 = 23°$. This is because of the combined effects of both a reduced R_1 and R_2 reflection component as a result of total internal reflection, as schematically indicated in Fig. 4(f).

3.3. Discussion

Previous experimental work shows that high efficiency perovskite / silicon tandem devices with silicon texture features of 1 to 2 μm and a steepness more than 23° ($\chi_2 > 23°$), can be fabricated in reality by means of blade-coating or solution processing of the perovskite layer [15,16]. It also shows that this perovskite layer tends to 'smoothen' the silicon texture, reducing the front texture

Optics EXPRESS

steepness such that $\chi_1 < \chi_2$. In the contour plots of Fig. 4, this represents the parameter space top/left of the main diagonal.

Figure 5(a) shows the simulation results of the encapsulated tandem with the optimum texture $\chi_1 = \chi_2 = 23°$. Absorptance in perovskite and silicon are indicated as solid red and blue lines, respectively. The dashed lines show the corresponding absorptances for the front-side flat reference case. Because perovskite absorption mainly benefits from the reduction of reflection component R_1, it mostly gains in the 350 to 500 nm wavelength range. The silicon absorption on the other hand mainly benefits from the reduction of reflection component R_2, and mostly gains in the 750 to 1150 nm wavelength range.

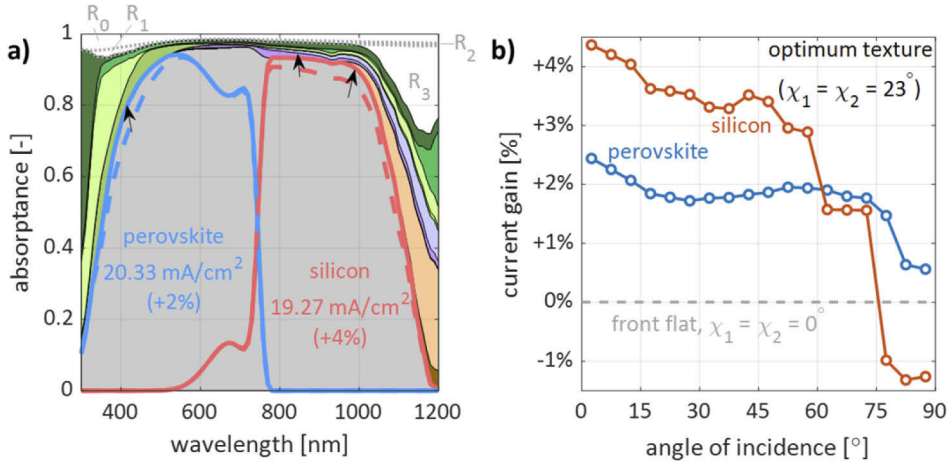

Fig. 5. a) Simulated reflectance (white) and absorptance in each layer (colors match Fig. 1(a)) as a function of wavelength, for encapsulated tandem with optimum texture ($\chi_1 = \chi_2 = 23°$). Blue and red lines represent useful absorptance in perovskite and silicon, with dashed lines for the front flat ($\chi_1 = \chi_2 = 0°$) reference case. b) Gain in implied photocurrent for perovskite (blue line) and silicon (red line) absorber layers in tandem with optimum texture, relative to front-side flat reference, as a function of the angle of incidence.

All simulation results presented thus far, assume that the incoming sunlight hits the tandem perpendicularly, i.e. at a 0° angle of incidence. The simulation of the encapsulated tandems, both with optimum texture ($\chi_1 = \chi_2 = 23°$) and the flat reference, were repeated for incident angles ranging from 2.5° to 87.5°. Figure 5(b) shows that the implied photocurrent gains, both in perovskite (blue line) and silicon (red line) are robust, and remain larger than +1.5% up to a very large incident angle of 75°.

It is evident that introducing front-side texture, results in gains in implied photocurrent in perovskite and silicon that are different, e.g. +2% in perovskite and + 4% in silicon. We consider two-terminal tandems that have their current limited by the sub-cell with the lower current. However, the expected gain in the current of the tandem as a whole is not the lower of the two gains (+2%), but approximately the average of both (+3%). This is because the perovskite thickness can be tuned to attain matching between top and bottom cell current. A more detailed argumentation is presented in supplement S4.

4. Conclusions

The front surface texture of a perovskite / silicon tandem must be sufficiently gentle to allow deposition of an efficient perovskite top cell, yet be optically efficient. We demonstrated experimentally that a tandem with a gentle texture steepness of 10° can achieve an efficiency as high as 28.6%. We then performed an extensive texture steepness optimization in which

Optics EXPRESS

we independently vary the texture steepnesses at both the front and rear side of the perovskite layer. This showed that for *unencapsulated* tandems, a gentle texture with a 20° steepness at the perovskite rear and flat front side, enhances the photocurrent of the silicon absorber by more than 3%. It does so by exploiting total internal reflection at the perovskite / air interface. In *encapsulated* tandem devices, total internal reflection at the glass / air interface can be exploited as well. A maximum total useful photocurrent gain of over 4% can be obtained with a gentle texture that has a steepness of 23°, both at the perovskite front and rear.

Funding. New Energy and Industrial Technology Development Organization; H2020 Societal Challenges.

Acknowledgments. The authors would like to acknowledge the financial support partially by the EU H2020 program for the SOLAR-ERA.net BOBTANDEM project, and partially by the New Energy and Industrial Technology Development Organization (NEDO) under the Ministry of Economy, Trade and Industry (METI).

Disclosures. The authors declare no conflict of interest.

Data availability. Data underlying the results presented in this paper are not publicly available at this time but may be obtained from the authors upon reasonable request.

Supplemental document. See Supplement 1 for supporting content.

References

1. E. Yablonovitch, "Statistical ray optics," J. Opt. Soc. Am. **72**(7), 899–907 (1982).
2. S.C. Baker-Finch and K.R. McIntosh, "Reflection distributions of textured monocrystalline silicon: implications for silicon solar cells," Prog. Photovolt: Res. Appl. **21**(5), 960–971 (2013).
3. P. Campbell, "Light trapping in textured solar cells," Sol. Energy Mater. **21**(2-3), 165–172 (1990).
4. J. Werner, B. Niesen, and C. Ballif, "Perovskite/silicon tandem solar cells: marriage of convenience or true love story? – An overview," Adv. Mater. Interfaces **5**(1), 1700731 (2018).
5. "World record again at HZB: Almost 30% efficiency for next-generation tandem cells," https://www.helmholtz-berlin.de/pubbin/news_seite?nid=23248;sprache=en, Nov. 2021.
6. A. Al-Ashouri, E. Kohnen, B. Li, A. Magomedov, H. Hempel, P. Caprioglio, J.A. Marquez, A.B. Morales Vilches, E. Kasparavicius, J.A. Smith, N. Phung, D. Menzel, M. Grischek, L. Kegelmann, D. Skroblin, C. Gollwitzer, T. Malinauskas, M. Jost, G. Matic, B. Rech, R. Schlatmann, M. Topic, L. Korte, A. Abate, B. Stannowski, D. Neher, M. Stolterfoht, T. Unold, V. Getautis, and S. Albrecht, "Monolithic perovskite/silicon tandem solar cell with >29% efficiency by enhanced hole extraction," Science **370**(6522), 1300–1309 (2020).
7. A. Richter, M. Hermle, and S.W. Glunz, "Reassessment of the Limiting Efficiency for Crystalline Silicon Solar Cells," IEEE J. Photovoltaics **3**(4), 1184–1191 (2013).
8. K. Yoshikawa, H. Kawasaki, W. Yosida, T. Irie, K. Konishi, K. Nakano, T. Uto, D. Adachi, M. Kanematsu, H. Uzu, and K. Yamamoto, "Silicon heterojunction solar cell with interdigitated back contacts for a photoconversion efficiency over 26%," Nat. Energy **2**(5), 17032 (2017).
9. M. Fischer, M. Woodhouse, S. Herritsch, and J. Trube, "International Technology Roadmap for Photovoltaic (ITRPV)," (2021).
10. M. Jost, E. Kohnen, A.B. Morales-Vilches, B. Lipovsek, K. Jaeger, B. Macco, A. Al-Ashouri, J. Krc, L. Korte, B. Rech, R. Schlatmann, M. Topic, B. Stannowski, and S. Albrecht, "Textured interfaces in monolithic perovskite/silicon tandem solar cells: advanced light management for improved efficiency and energy yield," Energy Environ. Sci. **11**(12), 3511–3523 (2018).
11. N. Tucher, O. Hohn, J.N. Murthy, J.C. Martinez, M. Steiner, A. Armbruster, E. Lorenz, B. Blasi, and J.C. Goldschmidt, "Energy yield analysis of textured perovskite silicon tandem solar cells and modules," Opt. Express **27**(20), A1419–A1430 (2019).
12. M. Filipic, P. Loper, B. Niesen, S. de Wolf, J. Krc, C. Ballif, and M. Topic, "CH3NH3PbI3 perovskite / silicon tandem solar cells: characterization based optical simulations," Opt. Express **23**(7), A263–A278 (2015).
13. F. Sahli, J. Werner, B.A. Kamino, M. Brauniger, R. Monnard, B. Paviet-Solomon, L. Barraud, L. Ding, J.J. Diaz Leon, D. Sacchetto, G. Cattaneo, M. Despeisse, M. Boccard, S. Nicolay, Q. Jeangros, B. Niesen, and C. Ballif, "Fully textured monolithic perovskite/silicon tandem solar cells with 25.2% power conversion efficiency," Nat. Mater. **17**(9), 820–826 (2018).
14. K. Jaeger, J. Sutter, M. Hammerschmidt, P.I. Schneider, and C. Becker, "Prospects of light management in perovskite/silicon tandem solar cells," Nanophotonics **10**(8), 1991–2000 (2021).
15. B. Chen, Z. J. Yu, S. Manzoor, S. Wang, W. Weigand, Z. Yu, G. Yang, Z. Ni, X. Dai, Z. Holman, and J. Huang, "Blade-coated perovskites on textured silicon for 26% efficient monolithic perovskite/silicon tandem solar cells," Joule **4**(4), 850–864 (2020).
16. Y. Hou, E. Aydin, M. De Bastiani, C. Xiao, F.H. Isikgor, D.J. Xue, B. Chen, H. Chen, B. Bahrami, A.H. Chowdhury, A. Johnston, S.W. Baek, Z. Huang, M. Wei, Y. Dong, J. Troughton, R. Jalmood, A.J. Mirabelli, T. G. Allen, E. van Kerschaver, M. I. Saidaminov, D. Baran, Q. Qiao, K. Zhu, S. de Wolf, and E.H. Sargent, "Efficient tandem solar cells with solution-processed perovskite on textured crystalline silicon," Science **367**(6482), 1135–1140 (2020).

Optics EXPRESS

17. R. Santbergen, T. Meguro, T. Suezaki, G. Koizumi, K. Yamamoto, and M. Zeman, "GenPro4 Optical Model for Solar Cell Simulation and Its Application to Multijunction Solar Cells," IEEE J. Photovoltaics **7**(3), 919–926 (2017).
18. N. Tucher, J. Eisenlohr, P. Kiefel, O. Hohn, H. Hauser, M. Peters, C. Muller, J.C. Goldschmidt, and B. Blasi, "3D optical simulation formalism OPTOS for textured silicon solar cells," Opt. Express **23**(24), A1720–A1734 (2015).
19. B. Lipovsek, J. Krc, and M. Topic, "Optical model for thin-film photovoltaic devices with large surface textures at the front side," Informacije MIDEM **41**, 264–271 (2011).
20. R. Santbergen, R. Mishima, T. Meguro, M. Hino, H. Uzu, J. Blanker, K. Yamamoto, and M. Zeman, "Minimizing optical losses in monolithic perovskite/c-Si tandem solar cells with a flat top cell," Opt. Express **24**(18), A1288–A1299 (2016).
21. S. Queisser, K. de Keersmaecker, T. Borgers, E. Wefringhaus, D. Nagel, B.U. Sander, M. Loehmann, M. Weber, and F. Delahaye, "Inline single side polishing and junction isolation for rear side passivated solar cells," *Proceedings of the 24th European Photovoltaic Solar Energy Conference, Hamburg, Germany* (2009).